



**Porous carbon spheres and monoliths: morphology controlling, pore size tuning and their applications as Li-ion battery anode materials**

Journal:	<i>Chemical Society Reviews</i>
Manuscript ID:	CS-TRV-02-2014-000071.R1
Article Type:	Tutorial Review
Date Submitted by the Author:	26-Mar-2014
Complete List of Authors:	Roberts, Aled; University of Liverpool, Chemistry Li, Xu; Institute of Materials Research and Engineering, Zhang, Haifei; University of Liverpool, Department of Chemistry

**Porous carbon spheres and monoliths: morphology controlling, pore size tuning and their applications as Li-ion battery anode materials**

*Aled D. Roberts<sup>a,b</sup>, Xu Li<sup>\*b</sup> and Haifei Zhang<sup>\*a</sup>*

a) Department of Chemistry, University of Liverpool, Liverpool, UK, L69 7ZD. Email:

zhanghf@liv.ac.uk.

b) Institute of Materials Research and Engineering, A\*STAR, Singapore, 117602. Email: x-

li@imre.a-star.edu.sg

*Keywords: Hierarchically porous carbon, carbon spheres, carbon monolith, Lithium-ion battery, anode materials*

## Abstract

The development of the next generation of advanced lithium-ion batteries (LIBs) requires new & advanced materials and novel fabrication techniques in order to push the boundaries of performance and open up new and exciting markets. Structured carbon materials, with controlled pore features on the micron and nanometer scales, are explored as advanced alternatives to conventional graphite as the active material of the LIB anode. Mesoporous carbon materials, carbon nanotubes-based materials, and graphene-based materials have been extensively investigated and reviewed. Morphology control (*e.g.*, colloids, thin films, nanofibrous mats, monoliths) and hierarchical pores (particularly the presence of large pores) exhibit increasing influence on LIB performance. This *tutorial review* focuses on the synthetic techniques for porous carbon spheres and carbon monoliths, including hydrothermal carbonization, emulsion templating, ice templating and new developments in making porous carbons from sustainable biomass and metal-organic framework templating. We begin with a brief introduction to LIBs, defining key parameters and terminology used to assess the performance of anode materials, and then address synthetic techniques for the fabrication of carbon spheres & monoliths and the relevant composites, followed respectively by a review of their performance as LIB anode materials. The review is completed with a prospective view on the possible direction of future research in this field.

## Key learning points

- A general introduction to lithium ion battery and electrode performance evaluation
- An outline of the most significant synthetic methodologies for the fabrication of carbon spheres and porous carbon monoliths
- A review of the performance of such materials as anode materials for the lithium-ion battery
- An outlook for the future direction of research in such fields

## 1. Introduction

With an ever increasing global population and growing energy demand *per capita*, there is an unprecedented drive to develop renewable energy technologies to mitigate the worst effects of climate change and alleviate pressure on rapidly depleting resources. The continual development of renewable energy sources, such as solar- and wind- based energy, has made up a large part of this technological drive. However, without a low-cost and efficient energy storage system to regulate the irregular and intermittent output, their full utility cannot be exploited. Advanced energy storage systems with high energy and power outputs at relatively low cost are also required to facilitate the transition from petroleum-based fuels to electric and hybrid-electric systems for automotive transport. Furthermore, with ever growing demand for portable consumer electronic devices such as smart-phones, tablet computers and laptops, there is a large market-driven pressure to develop smaller, lighter and higher capacity portable power sources without incurring excessive costs. Advanced batteries are currently regarded as the most feasible energy storage systems to satisfy these challenges.<sup>1</sup>

Since the development of the rechargeable (or secondary) lithium-ion battery (LIB) in the early 1990's, graphitic carbon has been predominantly employed as the anode material of choice due to a number of desirable characteristics, which include low cost, easy processability and chemical stability, in addition to having a desirable electrochemical profile.<sup>2</sup> The shortcomings of graphite, namely limited energy and power output per unit mass or volume, are holding back the development of certain high-tech industries such as electric vehicles and stationary energy storage.<sup>1</sup> New carbon and carbon-composite materials are therefore being actively perused for high performance LIBs.<sup>1-5</sup>

The development of advanced carbon-based materials with well-defined characteristics on the micro- and nano-scale has been a very active area of research recently.<sup>4-6</sup> Novel carbon nanostructures with remarkable physical and chemical properties, such as fullerenes, single- and multiwalled carbon nanotubes, and graphene, have been of particular interests.<sup>6</sup> Carbon spheres and ordered porous monoliths are other classes of nanostructured carbon materials, and have shown good promise not only for application as alternative LIB anodes, but also for supercapacitor electrodes, H<sub>2</sub> storage, catalyst supports, and as materials for separation and water-purification.<sup>4-7</sup> Different techniques are employed to vary physical and chemical characteristics (such as microstructure, crystallinity and

porosity) of carbon materials in order to tune their electrochemical performance.<sup>2</sup> A number of excellent reviews on mesoporous carbons, CNT-based, and graphene-based materials have been published, particularly for energy storage applications. Interested readers are referred to the electronic supplementary information for more articles/reviews on these topics. However, the review papers on fabrication of porous carbon spheres and carbon monoliths with techniques such as emulsion-templating and ice templating for energy storage are very limited.

The aim of this *tutorial review* is to provide a comprehensive introduction to the fabrication techniques for carbon spheres and porous carbon monoliths with an emphasis on relatively new and promising developments. The use of such materials as anodes for LIBs will be addressed to show how the morphology, pore size and material composition may influence LIB performance. This review is organized as follows: Firstly, introducing LIB, anode materials, and how the performance of anodes may be assessed; Secondly, describing the techniques used to prepare carbon spheres, and the use of carbon spheres as anodes; Thirdly, reviewing methods for the fabrication of porous monoliths with a focus on macroporous structures (*e.g.*, by emulsion templating and ice templating) and some new development in preparing carbon materials (*e.g.*, the use of biomass and metal-organic framework (MOF) templating). Subsequently, the performance of these materials as LIB anodes is discussed. We complete the review with conclusion and an outlook for the future development in this research field.

## 2. Lithium-ion battery

A battery is a unit or device that transforms chemical energy to electric energy and supply electrical energy via terminals/contacts.<sup>8</sup> There are two types of batteries: primary batteries and secondary (or rechargeable) batteries. A primary battery generates energy to be used until exhausted, and then discarded. Primary batteries are assembled in the charged state. For a secondary battery, after being discharged, the electrical energy can be restored by applying an electric current flowing in the direction opposite to the flow of current when the cell was discharged. The secondary batteries are usually assembled in the discharged state. Generally, rechargeable batteries have lower energy storage capability than primary ones. The most widely investigated rechargeable batteries are probably LIBs. LIBs reversibly interconvert electrical and chemical energy via a ‘rocking-chair’ mechanism, and

works through the reversible insertion/extraction of Li-ions between redox-active host materials (*i.e.*, the electrodes), which are separated by a Li-ion conducting (but electrically insulating) medium (*i.e.*, the electrolyte) (Fig. 1). The active material in the negative electrode (or anode) of a typical LIB is graphitic carbon, and the most common active material for the positive electrode (or cathode) is  $\text{LiCoO}_2$  (although other cathode materials such as  $\text{LiFePO}_4$  and  $\text{LiMn}_2\text{O}_4$  are also used). The respective equations for the materials are as follows:

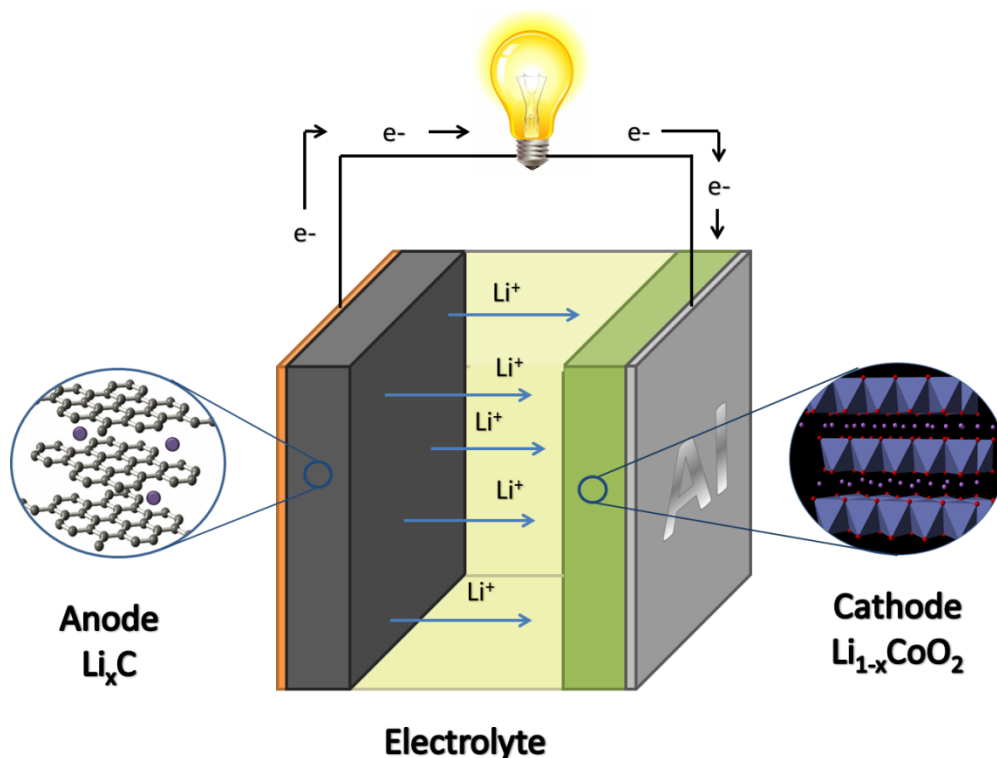
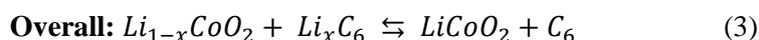
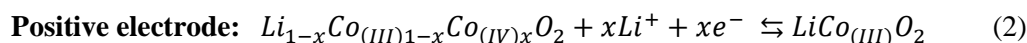
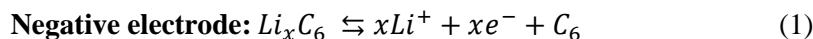


**Fig. 1** Schematic representation of a lithium-ion battery undergoing discharge.

Migration of the  $\text{Li}^+$  ions from the anode to the cathode thus occurs via the ionically conducting electrolyte, along with transport of electrons via an external circuit connecting the electrodes.<sup>9</sup> This reaction is driven by the electrochemical potential difference (or voltage) between the electrodes, and the resultant flow of electrons (or current) may be utilized to perform useful work.<sup>9</sup> To charge the cell,

an external potential difference (of the same polarity) is placed between the electrodes which drives the process in reverse.

## 2.1 Electrode performance evaluation for lithium-ion battery

There are a number of factors to consider when evaluating the performance of potential LIB electrode materials. The most important factors can vary, depending on the desired applications of the batteries. For instance, batteries intended for use in electric vehicles may require a high power output, fast charging rate and high specific energy, whereas batteries for stationary energy storage may place more value on low cost and longevity. Some of the principle factors to be considered when assessing the performance of a LIB electrode material are described below. The electrode can be prepared by active materials (anode or cathode material), conductive agent (if the active material is poorly conductive), binder (powdered active materials need to be bound together) and current collector. For LIBs, the electrolyte is typically a combination of lithium salts, such as  $\text{LiPF}_6$ ,  $\text{LiBF}_4$ , or  $\text{LiClO}_4$ , in an organic solvent such as ethylene carbonate. A separator (normally porous membrane) is within the electrolyte to separate the cathode and the anode.<sup>9</sup>

### Charge capacity and energy density

The total energy stored in a given electrode material is obviously an important factor, and can be quoted as the energy or the charges per unit mass (or specific energy, in  $\text{Wh kg}^{-1}$ ), or energy per unit volume (energy density, in  $\text{Wh L}^{-1}$ ). The theoretic energy capacity ( $C^{th}$ ) can be calculated by:<sup>10</sup>

$$C^{th} = nF/M \quad (4)$$

Where  $n$  is the number of moles of electrons during the electrochemical reaction,  $F$  is Faraday constant, and  $M$  is the molecular weight of the active electrode material. For instance, fully intercalated graphite has a stoichiometry of  $\text{LiC}_6$ , meaning there is 1 mole of charge carriers (equal to  $F$ , or 96,485 C) per mole of  $\text{C}_6$ . Since the  $M$  of  $\text{C}_6$  is  $72 \text{ g mol}^{-1}$ , the charge per gram of  $\text{C}_6$  is simply  $F/72$ , or 1340 C. Conversion into  $\text{mAh g}^{-1}$  (given that  $1 \text{ mAh} = 3.6 \text{ C}$ ) gives the result of  $372 \text{ mAh g}^{-1}$  as the theoretical capacity of graphite, an often quoted value in the literature.

The energy density of an electrode material is equal to the product of its voltage and charge per unit (or charge capacity), given by equation:

$$\text{Energy Density} = E \cdot C \quad (5)$$

The theoretical energy density is the product of  $C^{\text{th}}$  and the open-circuit voltage, and is often expressed in units of  $\text{Wh kg}^{-1}$ . Thus, the energy stored by an electrode material can be enhanced by either increasing the charge capacity ( $C$ , in  $\text{Ah g}^{-1}$  or  $\text{C g}^{-1}$ ,  $1 \text{ Ah} = 3600 \text{ C}$ ), or increasing the potential difference between the electrodes ( $E$ ).

### Power density

The power is the rate in which an electrode material can deliver energy, and is also typically quoted per unit mass ( $\text{W kg}^{-1}$ ) or per unit volume ( $\text{W L}^{-1}$ ) as specific power or power density, respectively. Power is the product of the current  $I$  (in A) and electrical potential difference  $E$  (in V) as given by the equation:<sup>9</sup>

$$P = IE \quad (6)$$

### Rate capability

The current output of an electrode  $I$  (in A, where  $1 \text{ A} = 1 \text{ C s}^{-1}$ ), is the rate of flow of charge and dictates how quickly an electrode material can be charged and discharged. When a high current is drawn from a cell, the power should theoretically increase proportionally, according to equation (6). This is not always the case however since, at high current densities, factors such as internal resistances and rate-limiting kinetics (known as polarization effects) cause a drop in electrical potential and thus a fall in power and energy.<sup>9</sup> The performance of materials at high current density, or rate capability, is thus another important factor which should be considered.

It should be noted here that the current output can also be expressed in terms of its  $C_{\text{rate}}$ , where a rate of 1 C is the current required to completely discharge a cell in 1 h, whereas a C-rate of 2 C is the current at which a battery would be fully discharged in 0.5 h. For making comparisons between different electrode materials, it is more convenient to quote the current density rather than the  $C_{\text{rate}}$ , since the former is independent of total capacity whereas the latter is not.

### Reversible and irreversible capacity

Upon the first charging cycle of a LIB there is an irreversible capacity loss (or  $C_{\text{irr}}$ ) associated with electrolyte reduction at the anode-electrolyte interface, which permanently consumes  $\text{Li}^+$  ions (and are thus unavailable as charge carriers).<sup>13</sup> Further reduction on subsequent cycles, and hence further capacity loss, is suppressed. This is because the initial process acts to form a stable passivation layer

(known as the solid electrolyte interface, or SEI), which, being permeable to  $\text{Li}^+$  ions but not to the electrolyte, acts as a barrier to further degradation.<sup>13</sup> Thus the initial reversible and irreversible capacities (denoted  $C_{\text{rev}}$  and  $C_{\text{irr}}$  respectively) are other important factors for the assessment of an electrode material. The value for  $C_{\text{irr}}$ , which for the abovementioned reasons is proportional to the anode-electrolyte interface, is therefore correlated to the surface area of the materials.

### Cycle stability

After the first charge/discharge cycle, and the inherent loss of capacity associated with the formation of the SEI layer, the capacity retention on subsequent cycles is another factor to consider. This is usually termed cycle life; and is the number of times a battery can be charged/discharged whilst still maintaining a reasonable capacity. The average capacity retention over a number of cycles is usually termed the cycle stability. Coulombic efficiency can be defined as the ratio of discharge capacity to charge capacity at the same cycle. It is an indication of the extent of irreversible capacity or the initial cycle stability. The cycle stability is related to the structural and chemical stability of the electrode materials.<sup>11</sup>

### Voltage profile

The electrical potential  $E$  (or voltage, in V) at which electrode materials undergo charge and discharge is not constant, but varies depending on the extent and conditions of these processes. Graphite typically has a fairly flat discharge profile, whereas the profile for disordered (or *turbostratic*) carbon is typically more sloped.<sup>9-11</sup> It is important to point out that the sloped voltage profiles from turbostratic carbons are not particularly desirable, especially for high-performance electronics. A flat working potential similar to that of graphite is preferred. A higher average voltage over the entire discharge profile also infers a higher energy density. It should be noted that as higher currents are drawn from an electrode material, internal resistances and rate limitations cause a drop in the potential, an effect known as polarization.<sup>9</sup> This diminishes the available power and energy from the cell. This is a significant issue associated with the current generation of LIB electrode materials since it limits their utility for high-power applications. These issues regarding polarization can be mitigated by minimising internal resistances and enhancing mass-transport,  $\text{Li}^+$  diffusion kinetics, and conductivity within the electrode.

In summary, the most important factors to consider when evaluating the performance of LIB anode materials may include energy density, reversible and irreversible capacity ( $C_{\text{rev}}$  and  $C_{\text{irr}}$ , respectively), cycle stability, rate performance, and voltage profiles. These factors are dependent on a number of chemical and physical properties associated with the material components and assembly of electrodes.

## 2.2. Carbon anode materials for the lithium ion battery

As mentioned in the introduction, graphitic carbon has been the anode material of choice since commercialisation of the LIB for many reasons, but is limited to low specific capacity and rate capability. Under ambient conditions, fully intercalated graphite has a stoichiometry of  $\text{LiC}_6$  – corresponding to a theoretical capacity of  $372 \text{ mAh g}^{-1}$ .<sup>3,11</sup> Carbons with disordered structures and no long-range order (or *turbostratic* carbon) have been shown to significantly exceed this theoretical capacity, suggesting that there are means, other than intercalation, by which Li can be stored in the carbon electrodes. Turbostratic carbon may be further classified as hard (non-graphitisable) or soft (graphitisable), depending on the microstructure.<sup>3</sup> Many groups have suggested models to explain this phenomenon of extra charge capacity, with theories that include formation of lithium multilayers on graphene sheets, entrapment of metallic lithium clusters in ultramicropores, extra storage capacity at edges of graphene layers, and the formation of  $\text{LiC}_2$ , C-H-Li or N-Li bonds.<sup>2,3,12</sup> But the exact mechanism is still unclear. Changing the structure and arrangement of the carbon at a microscopic scale can also have a profound effect on the performance. Porous carbon monoliths and sub-micron spheres, as will be discussed in the forthcoming sections, can enhance high-rate performance by overcoming issues associated with polarization.<sup>9</sup> Such changes are not without shortcomings. For instance, the  $C_{\text{irr}}$  is typically much higher (as a consequence of the relatively high H content and high surface area leading to greater SEI formation), and the voltage profile is generally sloped and lower on average than that of graphite.<sup>3</sup> Cost is also an issue. Graphite is a relatively low-cost and abundant material. Any contender would have to show superior performance without incurring excessive costs with regard to its precursor materials and method of fabrication.

The challenges for developing superior anode materials (and ideally industrially viable) are significant. In addition to tuning porosity and nanostructured morphology, another possibility is the use of certain lithium alloy forming materials, such as Sn, SnO<sub>2</sub> or Si, which have relatively high theoretical specific capacities of 994, 781, and 4200 mAh g<sup>-1</sup> respectively, as supplements to the carbon-based anodes.<sup>2-9</sup> Such alloys, on their own, suffer from significant problems as anode materials, including poor electrical conductivity and poor cycle stability associated with destructive volumetric expansion/contraction on charge/discharge. However, there have been many reports that the combination of such high capacity materials within a ‘stabilizing matrix’ (generally an inactive metal or carbon), can overcome such problems to an extent – with the stabilizing materials acting as a buffer against destructive volumetric changes, in addition to enhancing conductivity.

The remainder of this review describes the fields of carbon spheres, porous monoliths and their composites. The main and most significant synthetic methodologies are firstly described, followed by reviewing their performances as LIB anode materials. There is an additional introduction about recent progress in the new approaches of making porous carbon materials, *i.e.*, biomass as carbon precursor and MOF templating.

### 3. Synthesis of carbon spheres

Carbon spheres (CSs) can be synthesized *via* a number of different techniques, which vary in terms of process complexity, sphere size and size distribution, and crystallinity & microstructure of the resulting carbon.

#### 3.1 Chemical vapour deposition

A simple and common route for the preparation of CSs is via chemical vapour deposition (CVD). In this process, a gaseous carbon precursor (which could be formed by vaporisation, sublimation, or atomization of a solid or liquid source) is subject to high-temperature treatment, which induces decomposition, radical formation, and aggregation of the precursor molecules. The growth of these agglomerates via continued deposition and decomposition of the carbon precursor ultimately leads to CS formation.<sup>6,7</sup> Catalysts may also be employed in the CVD method for the fabrication of CSs, with

such processes generally referred to as catalytic-CVD mechanisms.<sup>7</sup> Here the catalysts may act as nuclei for the growth of CSs or as stimulants for the decomposition of the carbon precursors. Solid, hollow and composite CSs with a range of sizes, microstructures and morphologies may be prepared by the CVD and catalytic-CVD routes.

An early example of CS fabrication via a CVD process was reported by Qian *et al.*<sup>13</sup> Toluene was used as precursor to fabricate solid CSs with diameters ranging from about 200 to 1000 nm by varying the composition of the carrier gas. By additionally employing an anodic aluminium oxide (AAO) template, the authors found that the sphere sizes could be reduced further to about 60 nm.<sup>13</sup> Jin *et al.* later investigated the CVD route to CS formation in greater depth and were able to produce CSs from a wide range of precursors, including ethane, hexane, cyclohexane, benzene, toluene, and styrene.<sup>14</sup> The sizes of the spheres could be controlled to a degree by variation of certain process parameters such as feed rate, reaction time and pyrolysis temperature; in doing so, sphere diameters between about 50 and 1000 nm could be obtained.<sup>14</sup>

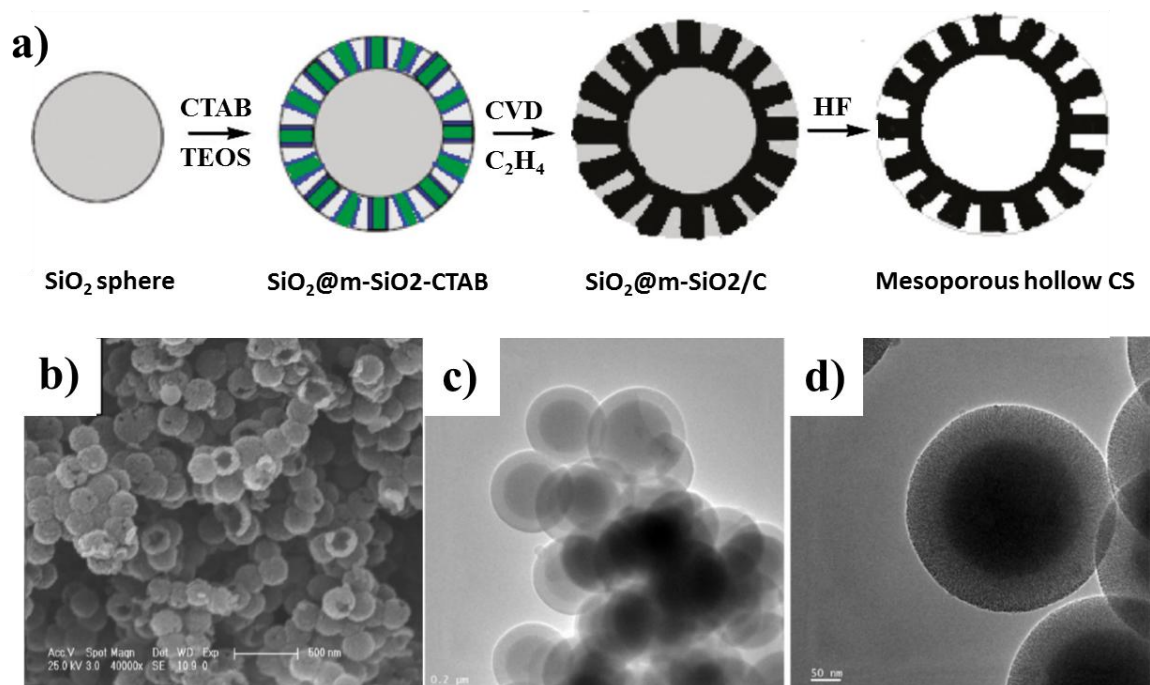


**Fig. 2** a) Schematic representation of the fabrication process for mesoporous hollow CSs. b) Scanning electronic microscopy (SEM) and c) & d) Transmission electronic microscopy (TEM) images of the hollow spheres. Adapted with permission from ref. 16. © 2011 American Chemical Society.

Hollow CSs can be fabricated via CVD using sacrificial sphere templates. For example, silica spheres were used as templates for benzene CVD and the subsequent removal of silica by HF etching produced hollow CSs.<sup>15</sup> More recently, hollow mesoporous carbon spheres were prepared by the CVD deposition of ethylene onto a mesoporous-silica@solid-silica template, before subsequent template removal (Fig. 2).<sup>16</sup> The resulting hollow CSs were about 220 nm in diameter with a mesoporous shell, a specific surface area of 771 m<sup>2</sup> g<sup>-1</sup>, and a relatively high degree of graphitization.

### 3.2. Hydrothermal carbonization

For the hydrothermal carbonization approach, carbohydrates and raw lignocellulosic biomass are converted into carbonaceous materials using mild processing temperatures (usually 100 – 300 °C) in sealed autoclaves under self-generated pressure. Carbon-rich precursors (*e.g.*, sugars, polysaccharides, and natural and renewable lignocellulosic biomass) are employed to facilitate high yield carbon formation. The precursors are dissolved in or mixed with a solvent (very often, water) in hydrothermal processes to induce partial or complete carbonization.<sup>17</sup>

Glucose is one of the frequently used precursors and others including xylose, maltose, sucrose, amylopectin, starch, hexose-based carbon sources, *etc.* Glucose was treated under relatively mild temperatures of about 160 – 180 °C without the subsequent high-temperature carbonization step.<sup>18</sup> The CSs produced were highly monodisperse, and the size control was obtained by varying reaction duration; with particles of 200, 500, 800, 1100 and 1500 nm produced as the reaction time increased from 2 to 4, 6, 8, and 10 h, respectively. By simple incorporation of precursor metal-salts or prepared colloidal nanoparticles into the glucose solution prior to carbonization, metal nanoparticles-encapsulated carbon spheres could be produced. Such a process may be translated to other materials in order to fabricate various carbon-composite spheres with novel properties for various applications.<sup>19</sup>

Templates could be introduced into the precursor solutions before hydrothermal treatment in order to produce composite or hollow spheres. With this process, it is important to form a uniform layer of carbon on the template while maintaining the discrete sphere morphology during the hydrothermal process. When silica spheres are used as templates, the surface hydrophobicity may

need to be tuned for uniform carbon coating. As reported by Joo *et al.*, treated SiO<sub>2</sub> particles with AlCl<sub>3</sub> were used as templates in a glucose hydrothermal process.<sup>20</sup> After carbonization and template removal with HF, hollow CSs were produced with diameters of about 340 nm and a high surface area of 788 m<sup>2</sup> g<sup>-1</sup>. Soft templates such as surfactant assembly could be also employed. For example, the simple incorporation of sodium dodecyl sulphate (SDS) into a glucose solution prior to hydrothermal treatment could result in hollow CSs.<sup>21</sup> The void size of the hollow spheres could be tuned from about 50 to over 1000 nm by varying the SDS concentration.

More recently,  $\alpha$ -cyclodextrin as carbon precursor was employed in the presence of block copolymer Pluronic F127 for hydrothermal reaction. After pyrolysis under argon at 900 °C, hollow carbon nanospheres were produced (Fig. 3).<sup>22</sup> As proposed by Yang *et al.*,  $\alpha$ -cyclodextrin could be threaded onto the F127 chains, which then formed micelles with a narrow size distribution, subsequently resulting in monodisperse CSs with controllable diameters between about 200 and 400 nm.<sup>22</sup>

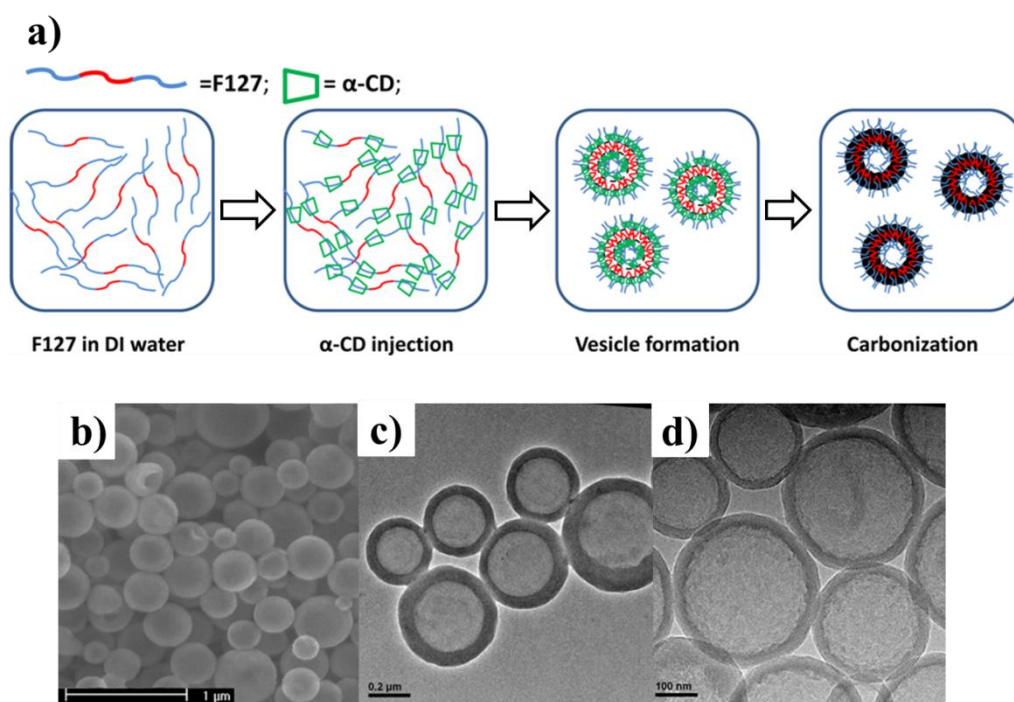


**Fig. 3** a) Schematic representation of the process where hollow CSs are prepared by the hydrothermal treatment of  $\alpha$ -cyclodextrin in the presence of Pluronic F-127. b) SEM and c) TEM images of the

spheres before carbonization, and d) the TEM image after carbonization. Adapted with permission from ref. 22. © 2013 American Chemical Society.

Hydrothermal routes are relatively simple, economical, and green for the fabrication of CSs of various sizes and characteristics. Challenges to their application as energy storage materials include difficulty in scale-up, fairly long reaction time, and the nature of the batch processes involved.

### 3.3. Other routes

There are other routes for the fabrication of CSs. The most common ones are arc discharge, laser ablation, and polymerisation-carbonization methods.<sup>7</sup> A brief outline of each is given below.

#### **Arc-discharge**

This process typically involves an electrical discharge between two high-purity graphite anodes within a chamber at a low-pressure and in inert atmosphere. High temperatures caused by the electrical arc sublime the carbon to form carbon vapour, which, upon cooling, condenses to form CSs. The CSs deposit on the cathode and the sides of the reactor before being collected. Due to low yields and relatively complex procedures, arc discharge is not regarded as an efficient method to fabricate CSs. It is often employed to fabricate more valuable carbon nanotubes in useful quantities.

#### **Laser ablation**

In a similar fashion to the arc discharge method, laser ablation works by vaporising a high-purity graphite source, and the vapour condenses to form CSs upon cooling. In a typical set-up, the graphite source is heated in a furnace under a flowing stream of inert gas. When a high-power laser ablates the carbon-source, the carbon vapour produced is then transported with the flowing gas to a cooled collector where the condensation of the carbon produces CSs.<sup>23</sup> This process is fairly complex and expensive, and typically employed to fabricate carbon nanotubes rather than CSs.

#### **Polymerisation-carbonization**

This method typically involves the formation of colloidal polymer spheres which, upon stabilization, drying, and pyrolysis, can be converted into CSs.<sup>24</sup> Different types of polymer precursors may be employed, including resorcinol-formaldehyde, polystyrene, poly(divinylbenzene) and

poly(phenylcarbene), among others. Various surfactants and block-copolymers, and hard templates can be employed in combination with the precursors to modify the size/porosity of the CSs and to generate core-shell structures respectively.

#### 4. Carbon Spheres as LIB Anode Materials

CSs have some desirable characteristics (*e.g.*, high specific capacity and good rate capability) to replace graphite as the LIB anode materials. Such advantages are likely down to a combination of factors, including: 1) short diffusion paths for  $\text{Li}^+$  ions; 2) tuneable porosity and high surface area to facilitate rapid charge transfer and minimize polarization effects; 3) tuneable microstructure, crystallinity, morphology, and composition of the carbon materials for high specific capacities. For further improvements in lithium storage capacity, it may be highly desirable to incorporate doped elements, metal oxides or alloys with enhanced bonding with Li or high Li storage capacity (*e.g.*, N-doped, H-doped, Si, Sn,  $\text{SnO}_2$ , MnO,  $\text{Fe}_3\text{O}_4$ , etc) into the carbon matrix.

Carbon nanospheres with diameters of  $\sim 500$  nm prepared by CVD pyrolysis of styrene were annealed at  $2800$  °C under Ar atmosphere.<sup>25</sup> The surface morphology of the CSs changed from smooth to polyhedral shape. The degree of graphitization and crystallinity substantially increased after the treatment. Electrochemical evaluation revealed an improved voltage profile and an increase in reversible capacity from  $220$  to  $280$  mAh  $\text{g}^{-1}$  for pre- and post- annealed CSs at a current density of  $30$  mA  $\text{g}^{-1}$ . In another relevant study, the researchers found that relatively small  $200$  nm CSs had much better performance in terms of discharge rate (power output) in comparison to much larger  $6$   $\mu\text{m}$  CSs prepared by following the same heat treatment.<sup>26</sup> This enhancement in performance could be attributed to a higher surface area resulting from small spheres and a reduced diffusion distance for  $\text{Li}^+$  ions within the bulk electrolyte. However, with this approach and the high temperature treatment, the energy capability is still low as it is not possible to go beyond the theoretical limit of graphite. To improve the capability, doped or composite CSs with small sizes and turbostratic disorder have been investigated to address this challenge.

N-doped CSs, with sizes ranging from about  $50$  to  $100$  nm, were prepared by polymerization and subsequent pyrolysis at  $900$  °C of polypyrrole nanospheres.<sup>27</sup> The electrochemical tests recorded a

high initial  $C_{\text{rev}}$  of about 420 mAh  $\text{g}^{-1}$  at a current density of 60 mA  $\text{g}^{-1}$ , which was relatively stable on cycling, decreasing to only about 380 mAh  $\text{g}^{-1}$  after 60 cycles. The spheres also had impressive high-rate performance, with a  $C_{\text{rev}}$  of 200 mAh  $\text{g}^{-1}$  at a current density of 3000 mA  $\text{g}^{-1}$ , suggesting that N-doping could be an effective means to improve the high-rate performance. Hydrogenated carbon nanospheres (diameters 40 -90 nm) were synthesized via a solvothermal route at low temperatures (60 – 100 °C) using  $\text{CHCl}_3$  as the carbon source and potassium as the reductant. The tests on these nanospheres as LIB anode exhibited a high discharge capacity (3539 mAh  $\text{g}^{-1}$  in the first cycle and 978 mAh  $\text{g}^{-1}$  after 50 cycles) and good cycling stability.<sup>28</sup> It was suggested that the electrochemical performance could be ascribed to the high percentage hydrogenation and nanoscale size. Li atoms could bind in the vicinity of H atoms in hydrogenated carbon materials, and the inserted lithium could transfer part of its 2s electron to a nearby hydrogen via a covalent bond. With these small nanospheres, the edges and defect sites could also prove more active for  $\text{Li}^+$  storage.

In addition to doped CSs, great efforts have been put into composite CSs to enhance the performance of LIB anode materials. Of these, Li-alloy-carbon core-shell structures have been of particular interest since the outer layer of carbon may overcome the problems faced by the alloy materials – namely poor electronic conductivity and pulverisation due to large volumetric change on charge and discharge (in which the carbon may act as both a conductivity enhancer and mechanical buffer). Hu *et al.* reported a hydrothermal method where Si nanoparticles (20 – 50 nm in diameter) were coated with a layer of carbon by hydrothermal treatment in the presence of glucose.<sup>19</sup> The hydrothermal treatment was found to induce oxidation of the Si nanoparticles surface, forming a  $\text{SiO}_x$  layer of about 3 – 5 nm in thickness between the Si and carbon. With addition of vinylene carbonate in the anode materials, reversible capacities as high as 1100 mAh  $\text{g}^{-1}$  were attained at a current density of 150 mA  $\text{g}^{-1}$ , which was stable even after 60 cycles.

$\text{SnO}_2$ @carbon is a type of core-shell materials which have been extensively investigated. In a recent study, rather than using a common hydrothermal route, polymerization of dopamine at room temperature was carried out in the presence of  $\text{SnO}_2$  nanospheres (diameters ~ 50 nm).<sup>29</sup> Polydopamine has a strong tendency to form coatings on various substrates. Carbonization of the resulting particles produced  $\text{SnO}_2$  nanospheres coated with N-doped multilayered graphitic carbon.

This SnO<sub>2</sub>@carbon as anode material showed a high capacity of 700 mAh g<sup>-1</sup> with a Coulombic efficiency of 99% after 100 cycles at a relatively high current density of 100 mA g<sup>-1</sup>.<sup>29</sup> The significant enhancement in capacity is attributed to the thin graphitic carbon coating which buffers the large volume change of SnO<sub>2</sub> clusters during the discharge-charge process and prevents their aggregation.<sup>29</sup> A one-pot hydrothermal method (employing sodium stannate and glucose) at 180 °C was used to prepare SnO<sub>2</sub>@carbon nanoclusters (diameters in the range of 25-35 nm and the size of SnO<sub>2</sub> core about 15-25 nm). Discharge capacity was measured as 1215 mAh g<sup>-1</sup> after 200 cycles at a current density of 100 mA g<sup>-1</sup>. The capacity was measured as 520 mAh g<sup>-1</sup> at the high current density of 1600 mA g<sup>-1</sup> and could be recovered to 1232 mAh g<sup>-1</sup> if the current density was back to 100 mA g<sup>-1</sup>.<sup>30</sup>

By following these preparation methods, it is possible to prepare metal oxide core and carbon shell particles in order to improve the different aspects of LIB performance.<sup>2-6</sup> A further focus is on the preparation and use of hollow CSs. Hollow spheres typically have higher surface areas than solid CSs, which is beneficial in terms of enhancing Li<sup>+</sup> transfer kinetics. Particularly, the carbon shell can significantly reduce the diffusion paths for Li<sup>+</sup> ions. However, the high surface areas may increase the instances of undesirable side-reactions with the electrolyte (SEI formation) – thereby potentially increasing C<sub>irr</sub> and reducing cycle stability. N-doped hollow CSs synthesised via CVD of benzene or acetonitrile onto silica spheres (diameter 460 – 1600 nm) gave C<sub>rev</sub> values of about 320 mAh g<sup>-1</sup> over 100 cycles (current density = 60 mA g<sup>-1</sup>) and high-rate performance of over 200 mAh g<sup>-1</sup> at a current density of 5000 mA g<sup>-1</sup>.<sup>15</sup> The sizes of the hollow CSs prepared by hydrothermal treatment of  $\alpha$ -cyclodextrin with F-127 were in the range of 200 – 400 nm, with a shell thickness of 50 -80 nm. A stable reversible capacity of about 450 mAh g<sup>-1</sup> over 75 cycles at a current density of 50 mA g<sup>-1</sup> was achieved as LIB anodes.<sup>22</sup>

Desirable nanoparticles have been incorporated into hollow CSs to provide higher LIB anode performance. For example, Sn nanoparticles (diameter ~ 100 nm) encapsulated in hollow CSs (diameter 500 nm and shell thickness 20 nm) were fabricated by a multiple-step procedure (Fig. 4).<sup>31</sup> When evaluated as a LIB anode material, the prepared Sn-encapsulated CSs showed a reversible capacity higher than 800 mAh g<sup>-1</sup> after 10 cycles and remained over 550 mAh g<sup>-1</sup> after 100 cycles, at a current density of 160 mA g<sup>-1</sup>. C<sub>irr</sub> was very high. However, the initial discharge capacity was about

1650 mAh g<sup>-1</sup>, meaning about half of the potential capacity (>800 mAh g<sup>-1</sup>) has been lost by the 10<sup>th</sup> cycle.

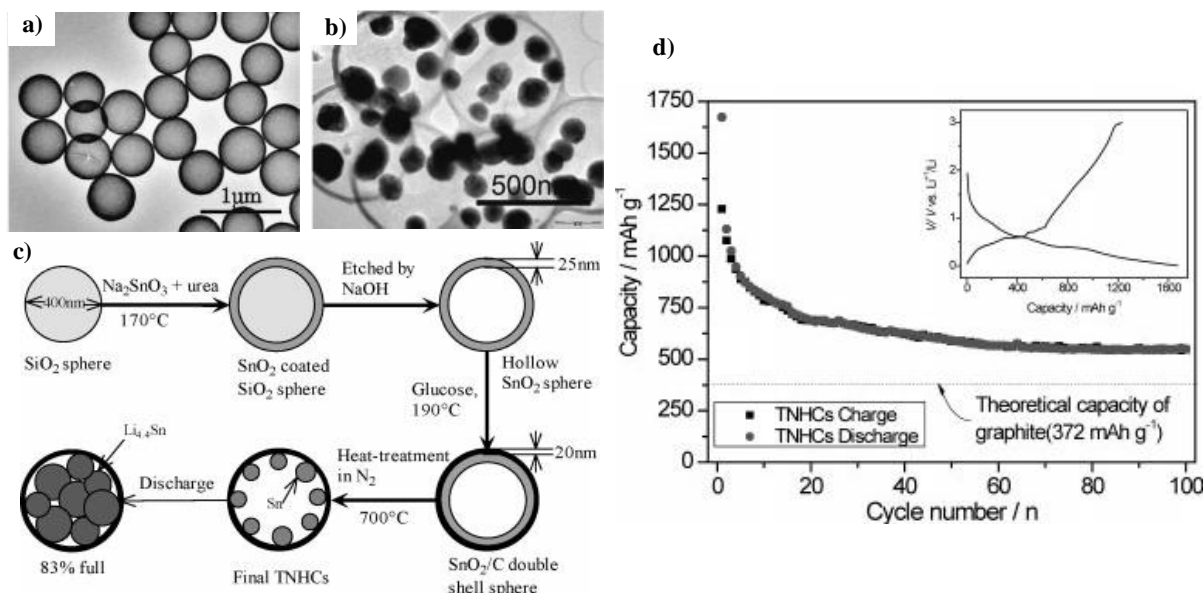


**Fig. 4** TEM images of a) the hollow CSs and b) the Sn-encapsulated hollow CSs. c) Schematic representation of the method employed and d) the cycling performance of the Sn-encapsulated hollow CSs. Adapted with permission from ref. 31. © 2008 Wiley-VCH.

There has been much investigation into the application of CSs as alternative LIB anode materials to graphite. Of the discussed methods for the fabrication of solid, hollow and composite CSs, the hydrothermal route seems the most viable due to its simplicity, low-temperature of operation, and the fact it may employ low-cost polysaccharides as carbon precursors. Soft templating routes are significantly more viable than hard templating methods, since the extra steps and use of harsh etching agents (typically HF or NaOH) to remove hard templates makes processing onerous. Composite-CSs have shown significant improvements in terms of anode performance over pure Li-alloy materials. However the associated problems with high  $C_{\text{irr}}$  values and poor cycle stability must be addressed and resolved.

## 5. Synthesis of porous carbon monoliths

There is no exact definition on “monolith”. Monoliths have been investigated and used in many research fields. In materials science, a monolith may be defined as a continuous block of material with a size upwards of 1 mm<sup>3</sup> and with a defined 3D shape. Commonly, the monoliths have the shapes of cylinder, cube, cuboid, *etc.* A sphere of different sizes is often called nanosphere, microsphere or bead, rather than a monolith. The most common route for the fabrication of porous carbon monoliths is via templating approaches. The templates can be classified as either hard templates such as silica or metal oxides or soft templates such as polymer, surfactant, or other non-inorganics. Liquid droplets may also be used as soft templates. For hard templating processes, the general procedure is to first impregnate a porous template with a carbon precursor which is subsequently converted to carbon and then remove the template usually by acid or strong base wash to give a porous carbon as the inverse replica of the original structure. Soft templating processes typically rely on the self-assembly of organic polymers or surfactants to direct the formation of a porous carbon structure. Soft templates may be readily removed by solvent washing, thermal decomposition, or different drying approaches.

### **5.1. Hard template routes**

The hard templates usually include inorganic colloids or pre-formed porous inorganic structures. For the inorganic colloidal templating, monodisperse silica spheres of different sizes are mostly used. Soft colloidal templates such as polymer spheres are also widely used in the colloidal templating approach. The monodisperse spheres assemble into ordered structures (usually by controlled solvent evaporation onto different substrates), before filling the voids with carbon precursors (Fig. 5). The precursors are then polymerized and carbonized to generate carbon composites. If carbon-rich polymers are used as precursors, the polymerization step may not be required. After removal of the templates by HF etching (or other routes), a carbon negative replica of the original colloidal crystal structure is produced.<sup>5</sup>

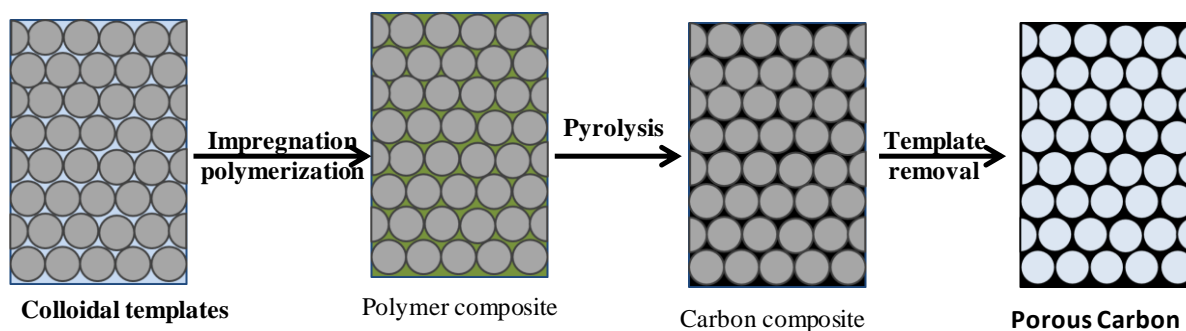


**Fig. 5.** Schematic representation of colloidal templating to produce ordered porous carbon materials. Both hard colloidal templates (*e.g.*, silica colloids) and soft templates (*e.g.*, polystyrene colloids) can be employed for this templating approach.

While most of the pre-formed porous inorganic materials may be used as templates, zeolites and mesoporous silica materials are mostly used to produce porous carbons.<sup>4</sup> The templating procedures, also known as nanocasting, are largely similar even when different porous structures are used. Fig. 6 shows a scheme depicting how mesoporous carbons are produced using mesoporous silica as templates.<sup>4</sup> Generally, a carbon precursor (*e.g.*, glucose, sucrose or monomers) is impregnated into the porous template and fills the pores. The impregnated structure may be subjected to a gelation/polymerization process or directly carbonized to produce silica/carbon composites. The silica is removed usually by acid etching to produce porous carbon materials.

A CVD process can be combined with a pre-formed porous structure as template for the preparation of porous carbon monoliths. Zhang and co-authors prepared three-dimensional (3D) graphene networks (3DGNs) by using Ni foam as a sacrificial template in a CVD process with ethanol as the carbon source.<sup>32</sup> Subsequently the Ni foam could be removed by an etching process. The metal oxide/3DGNs could be further prepared by electrochemical deposition of NiO,<sup>32</sup> or thermal decomposition with metal-organic frame works as precursors.<sup>33</sup>

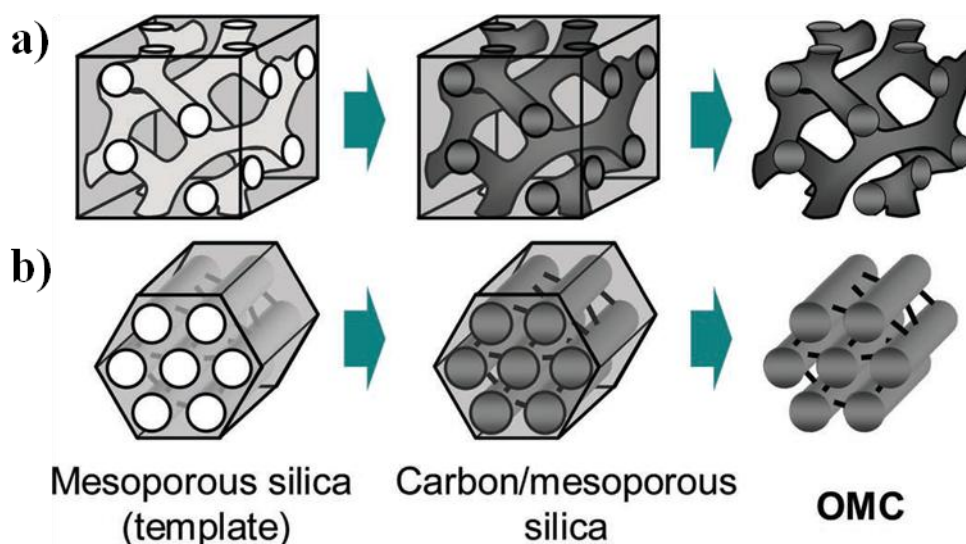


**Fig. 6.** Schematic representation of the process using pre-formed porous structures as templates to prepare porous carbons. The structures here specifically represent the use of mesoporous silica of a) MCM-48 and b) SBA-15 for the fabrication of ordered mesoporous carbons (OMCs). Adapted with permission from ref. 4. © 2012 Wiley-VCH.

## 5.2. Soft template routes

Alternative to hard templates, polymer colloids have been widely used as soft templates to produce porous carbon monoliths (Fig. 5). Among them, poly(methyl methacrylate) (PMMA) and polystyrene (PS) colloids are most commonly used. Unlike the silica templates, the polymer templates can be simply removed through washing by using a suitable solvent (*e.g.*, toluene, tetrahydrofuran) or simultaneous decomposition during the thermal treatment. For example, the close-packed arrays of colloidal PMMA templates could be formed by simple gravitational settling, before being soaked in a resorcinol-formaldehyde (RF) solution which acted as the carbon precursor.<sup>5</sup> Subsequent thermal polymerisation (85 °C) and carbonization (900 °C) induced crosslinking and carbonization of the RF gels respectively; the former process aids the mechanical stability and prevents melting during the latter. Carbonization also removed the PMMA templates, meaning there was no need for extra template-removing steps such as acid etching.

Surfactant assemblies have been widely used to produce mesoporous carbon materials. The cationic surfactant cetyltrimethylammonium bromide (CTAB) and the amphiphilic triblock

copolymers poly(ethylene oxide)-poly(propylene oxide)-poly(ethylene oxide) (particularly Pluronic P-123 and Pluronic F-127) are commonly used as soft templates while RF solutions are the mostly used carbon precursors. Thermally induced polymerization of the RF around the surfactant templates yields a rigid structure. Removal of the surfactant templates is performed by simple calcination or solvent-exchange, followed by carbonization to produce the mesoporous carbon.<sup>4,34</sup>

Both emulsion templating and ice templating can be regarded as soft template approaches. However, they are not reviewed as extensively as other templating approaches for the preparation of hierarchically porous carbon materials. Both techniques are explained and discussed in more detail in the following sections.

### **Emulsion templating**

An emulsion is a mixture of two immiscible phases where one is typically dispersed within the other in the form of droplets, *i.e.*, droplet phase and continuous phase. Generally there are two types of emulsion: oil-in-water (O/W) emulsion where the droplet phase is organic solvent while the continuous phase is water and water-in-oil (W/O) emulsion where water or aqueous solution is the droplet phase with the organic continuous phase. The number of droplets in an emulsion can be varied, normally expressed as the volume ratio of droplet phase to the continuous phase or the volume percentage of the droplet phase in the emulsion. When the volume percentage of the droplet phase in an emulsion is greater than 74.05%, this emulsion is called a high internal phase emulsion (HIPE) where the droplets are closely packed.<sup>35</sup> To form an emulsion, a suitable surfactant is generally required to stabilize the droplets dispersed in the continuous phase. Sometimes, a co-surfactant or co-solvent is added to improve the emulsion stability. In order to use emulsions as templates to prepare porous polymers, monomers & initiators are dissolved in the continuous phase and then polymerized while the emulsion structure is maintained (Fig. 7). Removal of the solvents from both the continuous phase and droplet phase produces emulsion-templated porous materials. Both O/W and W/O emulsions have been employed to produce a range of porous polymers and porous inorganic materials.<sup>35</sup> HIPEs as templates can generate highly interconnected porous materials (known as *polyHIPEs*) while an emulsion with low volume percentage of internal phase may produce porous materials with closed pores.

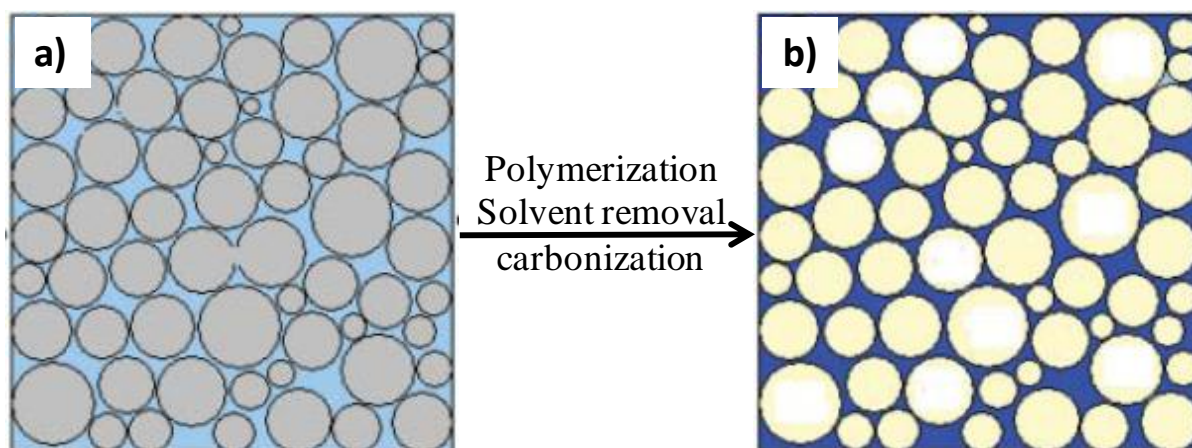


**Fig. 7** Schematic representation of emulsion-templating approach for porous carbon materials. a) Carbon-rich monomers/initiators are dissolved in the continuous phase while the solvent droplets are used as templates; b) After polymerizing the monomers in the continuous phase and removing the solvents from both continuous and droplet phase, the resulting porous polymer can then be carbonized to produce porous carbon.

Carbon-rich monomers (*e.g.*, acrylonitrile, furfural, RF) are usually employed to make emulsion-templated porous polymers which are then pyrolyzed to produce porous carbon monoliths. For example, acrylonitrile (AN) was used to form polyacrylonitrile (PAN)-based polyHIPE by crosslinking through copolymerization with divinylbenzene using W/O HIPE as template. Due to the miscibility of AN with water, a polyglycerol polyricinoleate surfactant was employed to stabilize the emulsion and both oil- and water-soluble initiators were utilized.<sup>36</sup> The pyrolyzed carbon had large macropores with the size of about 10  $\mu\text{m}$ , and a surface area of 26.5  $\text{m}^2 \text{g}^{-1}$ . In another attempt to use W/O emulsions as templates, styrene/divinylbenzene/vinylbenzyl chloride/span 80 (as surfactant) were used as the oil phase. The aqueous phase containing stabilizing salt  $\text{CaCl}_2 \cdot 6\text{H}_2\text{O}$  and  $\text{K}_2\text{S}_2\text{O}_8$  as initiator was emulsified into the oil phase. After polymerization and carbonization, highly interconnected macroporous structures were obtained (Fig. 8).<sup>37</sup> The resulting carbon monolith contained cellular pores of  $\sim 25 \mu\text{m}$ , disordered carbon with pore sizes  $< 100 \text{ nm}$ , and a surface area of 433  $\text{m}^2 \text{g}^{-1}$ .

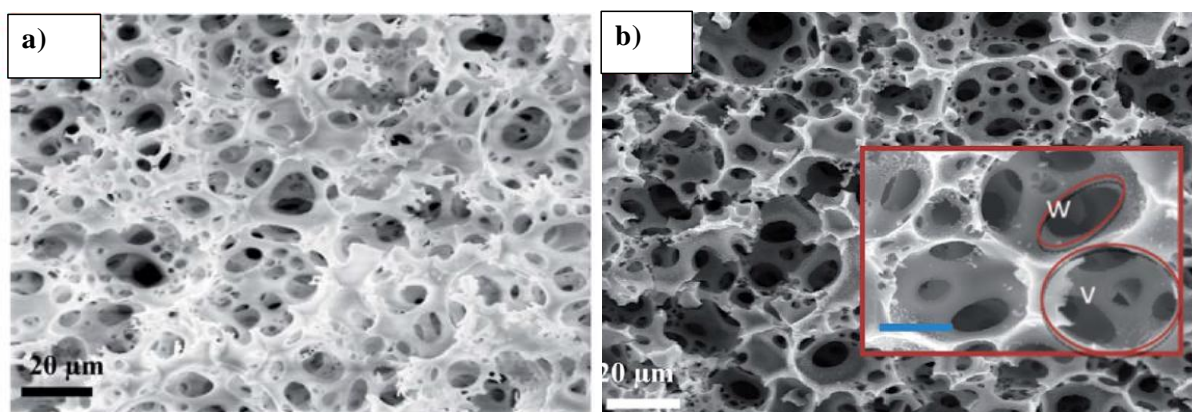


**Fig. 8** The SEM images of emulsion-templated porous polymer before a) and after carbonization b). The scale in the inset image of (b) is 10  $\mu\text{m}$ . Adapted with permission from ref. 37.

A hydrothermal carbonization approach was also employed to prepare emulsion-templated carbon monoliths. An O/W emulsion was firstly formed with furfural/phloroglucinol as precursors, Tween 80 as surfactant and  $\text{FeCl}_3$  as catalyst dissolved in the continuous hydroalcoholic mixture, and dodecane as the internal phase.<sup>38</sup> Gelation of the emulsion was required before transferring into an autoclave for hydrothermal carbonization. The resulting carbon-polyHIPEs showed good mechanical stability, electrical conductivity of  $300 \text{ S m}^{-1}$ , surface areas of up to  $730 \text{ m}^2 \text{ g}^{-1}$ , and total pore volumes of about  $0.313 \text{ cm}^3 \text{ g}^{-1}$ . Pre-formed polyHIPEs can also be used as templates to prepare porous carbon monolith. Brun *et al.* firstly prepared silica polyHIPE and then added into a RF prepolymer hydroalcoholic solution for impregnation.<sup>39</sup> The silica template was removed by HF etching either before or after pyrolysis at  $900 \text{ }^\circ\text{C}$  under Ar flow. The carbonaceous foams exhibited interconnected macro-/microporous pores (surface areas  $\sim 650 \text{ m}^2 \text{ g}^{-1}$ ), electrical conductivity of  $20 \text{ S cm}^{-1}$ , and excellent mechanical property (Young's modulus  $0.2 \text{ GPa}$  and toughness of  $13 \text{ J g}^{-1}$ ).

### Ice templating

Ice-templating is a facile process where a solution, suspension, or emulsion is being frozen and the frozen solvent is removed typically by freeze-drying (also called lyophilisation) to generate a highly interconnected macroporous structure.<sup>6,40</sup> The control of ice crystal size and growth orientation is

highly important for the resulting pore structures. As shown in Fig. 9, the solution may be randomly frozen (*e.g.*, by placing in a freezer) (Fig. 9a) or directionally frozen (*e.g.*, by dipping into liquid nitrogen at a controlled rate) where the growth of ice crystals are orientated (Fig. 9b). With the existence of temperature gradient during freezing, it is unlikely to produce a frozen sample with completely randomly distributed ice crystals. Generally, the higher temperature gradient and the faster freezing rate can generate frozen samples with smaller sizes of ice crystals. Addition of some polymers or inorganic salts may also modify the size crystals. During the freeze-drying process, the samples are kept frozen and the ice crystals are removed by sublimation under vacuum. It is possible that the frozen samples may partially melt. However, the freeze-drying rate should be sufficiently fast to remove the melted water immediately. Otherwise, the ice-templated structures may be damaged.

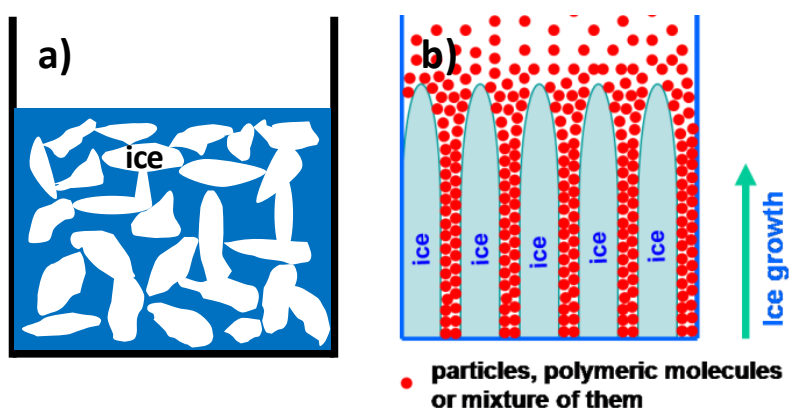


**Fig. 9** Schematic representation of ice crystals as templates. a) ice growth randomly; b) orientated ice growth (adapted with permission from *Adv. Mater.* 2007, **19**, 1529. © 2007 Wiley-VCH). When carbon-rich polymers are used, the ice-templated porous polymers can be carbonized to produce hierarchically porous carbon materials.

The ice-templating method has been applied to a wide range of systems to produce porous and fibrous structures of various materials.<sup>6,40</sup> Aqueous solutions or suspensions have been mostly used. To prepare porous carbon by ice templating, carbon-rich precursors should be used. For example, a renewable biopolymer lignin was utilized as a carbon precursor.<sup>41</sup> Instead of forming porous structures, the freeze-drying of the diluted polymer solutions could produce nanofibrous

structures.<sup>41,42</sup> Subsequent carbonization yielded a corresponding nanofibrous carbon mat, with surface areas of up to  $1250 \text{ m}^2 \text{ g}^{-1}$ .<sup>41</sup> Both ice templating and silica colloidal templating with glucose were used for the preparation of hierarchically porous carbons with tuneable porosity over the macro-, meso-, and micro-pore size domains.<sup>43</sup> The silica templates were removed by HF etching. The resulting carbons had ultrahigh specific pore volumes of  $\sim 11.4 \text{ cm}^3 \text{ g}^{-1}$  and were investigated for  $\text{CO}_2$  capture and as supercapacitor electrodes.

Due to their excellent properties, carbon nanotubes (CNTs) and graphene have been intensively investigated in recent years. Both CNTs and graphene are utilized in the ice-templating process for the preparation of materials with exciting applications.<sup>6</sup> Very often, CNTs or graphene are dispersed in aqueous medium stabilized with polymer to form composite materials. The high percentage of CNTs/graphene renders the materials electrically conductive. They could be used directly as electrodes with high performance.<sup>6</sup> It is also possible to prepare ice-templated porous CNTs or graphene materials. For example, partially reduced aqueous graphene-oxide (GO) suspensions were used in an ice-templating process to produce GO monoliths. Further reduction resulted in the corresponding graphene monoliths, which displayed unique mechanical properties – including very high elasticity and structural integrity under compression.<sup>44</sup>

Carbon cryogels are another type of materials which have been extensively investigated, involving freeze-drying processes where the frozen solvent crystals act as templates.<sup>45</sup> The general procedure is: (1) firstly the precursors are dissolved in water or hydroalcoholic mixture with a suitable catalyst; (2) gelation of the precursors occurs normally at mild temperatures; (3) the gel is frozen and the frozen solvent is removed by freeze-drying or solvent exchange; (4) the dry gel is carbonized in an inert atmosphere to produce carbon cryogels. The RF precursors are the mostly investigated to fabricate carbon gels.

### 5.3 Other progresses

Some exciting progresses have been made in recent years, although they are not exclusive to the preparation of porous carbon spheres or monoliths. We describe briefly here the use of biomass as

carbon precursors and metal-organic frame works (MOFs) as templates for the production of porous carbon materials.

### **Biomass as carbon precursors**

Carbon materials have been long synthesized from petroleum-derived compounds. Due to the approaching depletion of carbon deposits and wide concerns on climate change and environmental pollution, the use of renewable natural resources for industrial production (including carbon materials) has been eagerly sought after. Biomass is a raw material available in high quality and huge amount that can be regarded as a sustainable precursor for preparation of carbon materials. Hydrothermal carbonization is the main process used for this purpose.<sup>17</sup> Waste biomass from agriculture or certain industries may be more favoured in terms of the process sustainability. However, it remains a great challenge to produce valuable carbon materials from crude biomass. The pre-treatment of biomass or the compounds derived from biomass are normally required. These include lignin, cellulose, glucose, sucrose, *etc.* Depending on the type of the precursors and hydrothermal conditions, porous carbon spheres, nanofibers, composites and aerogels can be produced, which have found a wide range of applications, including as electrode materials.<sup>4,6,34</sup>

### **Metal-organic frameworks as templates**

MOFs are a type of crystalline porous materials via the linkage of metal ions and organic ligands. Most MOFs exhibit micropores of varied morphologies although great effort (*e.g.*, by ligand extension, combining the synthesis with surfactant templating) has been made to prepare mesoporous MOFs. Due to large number of metal ions and nearly unlimited types of organic ligands available, there are great opportunities to produce MOFs with desirable properties. Like the other types of porous materials, MOFs could be used as templates to fabricate porous carbons. Although a large number of MOFs are available, only a small fraction of MOFs (mainly Zn-based and Al-based MOFs) have been utilized so far.

Like zeolites or mesoporous silica, MOFs may be used as hard templates to prepare porous carbons. The procedure includes impregnation of a carbon precursor into MOFs, followed by carbonization and template removal. For example, furfuryl alcohol as a carbon precursor was

introduced into the micropores of a highly porous zeolite imidazole framework (ZIF-8,  $\text{Zn}(\text{MeIM})_2$ , MeIM = 2-methylimidazole). The polymerization and carbonization procedure generated a nanoporous carbon material with high surface area of  $3405 \text{ m}^2 \text{ g}^{-1}$ , high hydrogen storage (2.77 wt% at 77K and 1atm), as well as good electrochemical properties as an electrode material for electric double layer capacitors.<sup>46</sup>

Unlike zeolites, MOFs contain organic ligands. Many of the ligands are aromatic multicarboxylic acids that are carbon-rich precursors. With their intrinsic crystalline microporosity, MOFs can be directly carbonized to produce nanoporous carbons. For example, Lim *et al.* prepared a series of Zn-containing MOFs for direct carbonization. An interesting linear relationship between the Zn/C ratio of the MOFs and the surface area of the resulting carbon materials was observed.<sup>47</sup> There was no need to remove Zn or ZnO from the carbon materials. During the heating under Ar (or  $\text{N}_2$ ), ZnO was initially formed and then reduced to Zn with carbon at higher temperature. Higher carbonization temperature (*e.g.*,  $> 1000 \text{ }^\circ\text{C}$ ) treatment could remove Zn (boiling point  $907 \text{ }^\circ\text{C}$ ) by evaporation.<sup>47</sup> Other types of MOFs may be also employed to produce nanoporous carbon materials. By incorporating nanoparticles or metal-organic complexes into the pores of MOFs, nanoporous carbon composites can be fabricated by simple carbonization as well.

## 6. Porous carbon monoliths as LIB anode materials

Porous carbon monoliths have a number of desirable characteristics which make them attractive candidates as alternative LIB anode materials. Advantages of porous monoliths over powder materials can include: i) an interconnected carbon structure facilitating electron percolation and hence good electrical conductivity, ii) a hierarchy of pores to facilitate fast  $\text{Li}^+$  diffusion kinetics and hence good rate capability, iii) no need to use an electrochemically-inactive glue (as required for the powder sample), which would reduce overall specific capacity, vi) a high surface area for good electrode-electrolyte contact, inducing rapid charge transfer, and v) reduced solid-state diffusion of  $\text{Li}^+$  ions in the bulk material due to relatively thin pore walls. These features, along with the relatively high proportion of turbostratic carbon, can lead to materials with the values of specific capacity and rate capability far in excess than that of graphite. Disadvantages of such systems can, however, include

high  $C_{\text{irr}}$  due to excessive SEI formation (as a consequence of high surface area), relatively poor cycle stability, poor voltage profiles, and relatively complex processing which may infer high costs.

Zhou *et al.* fabricated ordered porous carbon monoliths, with high surface area values of  $1030 \text{ m}^2 \text{ g}^{-1}$  and pore sizes of about 4 nm, from a mesoporous SBA-15 silica template utilising glucose as the carbon precursor.<sup>12</sup> The material, termed CMK-3, when tested as an anode material for LIBs, displayed a very high and moderately stable  $C_{\text{rev}}$  of about  $1100 \text{ mAh g}^{-1}$ , falling to about  $850 \text{ mAh g}^{-1}$  after 20 cycles. However, this was accompanied with a large initial irreversible capacity loss of about  $2000 \text{ mAh g}^{-1}$ , which was primarily attributed to extensive SEI formation associated with the high surface area of the material. Ordered macroporous carbons prepared from colloidal templating have been widely investigated.<sup>5</sup> Macroscopic carbon monoliths with mesopores (7.3 nm) and macropores (1-4  $\mu\text{m}$ ) were prepared by using meso-/macroporous silica as a template and mesophase pitch as carbon precursor.<sup>48</sup> LIB anode performance evaluation revealed an initial reversible capacity of  $900 \text{ mAh g}^{-1}$  at a current density of  $180 \text{ mA g}^{-1}$ , which remained above  $500 \text{ mAh g}^{-1}$  after 40 cycles. A stable reversible capacity of  $260 \text{ mAh g}^{-1}$  at a very high current density of  $2600 \text{ mA g}^{-1}$  was observed. This was attributed to the hierarchy of pores providing favourable  $\text{Li}^+$  transfer kinetics. The reversible capacity decreased with decreasing H-content in the carbon samples. A nearly linear relationship was observed. This could be attributed to the Li-H-C interactions. For the same reason, a very high charge capacity was observed with the hydrogenated carbon nanospheres.<sup>28</sup>

Emulsion-templated carbon was tested as an anode material, showing a reversible capacity exceeding  $3.5 \text{ mAh cm}^{-2}$  at a current density of  $0.37 \text{ mA cm}^{-2}$ . There was no structure degradation observed after testing for 50 cycles.<sup>37</sup> For the porous carbonaceous monoliths prepared from silica polyHIPE template as LIB anode, a stable capacity of  $200 \text{ mAh g}^{-1}$  was achieved for the first 50 cycles at a current density of  $C/10$ .<sup>39</sup> Colloidal templating has been more often used to prepare hierarchically macroporous carbons. Ordered multimodal porous carbons (OMPCs) were prepared by dual polystyrene microsphere and silica nanosphere templating with furfuryl alcohol as carbon precursor (Fig. 10).<sup>49</sup> The material had a surface area of  $1120 \text{ m}^2 \text{ g}^{-1}$ , similar to that of CMK-3 (about  $1100 \text{ m}^2 \text{ g}^{-1}$ ).<sup>12</sup> However, the initial  $C_{\text{irr}}$  was far lower than that of CMK-3, at only  $671 \text{ mAh g}^{-1}$  (at a current density of  $100 \text{ mA g}^{-1}$ ). The  $C_{\text{rev}}$  was high at  $903 \text{ mAh g}^{-1}$  and relatively stable after 80 cycles

– falling by only about  $100 \text{ mAh g}^{-1}$ . The OMPCs maintained good performance even at the high current density of  $1000 \text{ mA g}^{-1}$ , with a specific capacity in excess of  $750 \text{ mAh g}^{-1}$ . The high rate performance may be attributed to superior  $\text{Li}^+$  diffusion kinetics due to the facile penetration and mobility of the electrolyte within the ordered macropores.

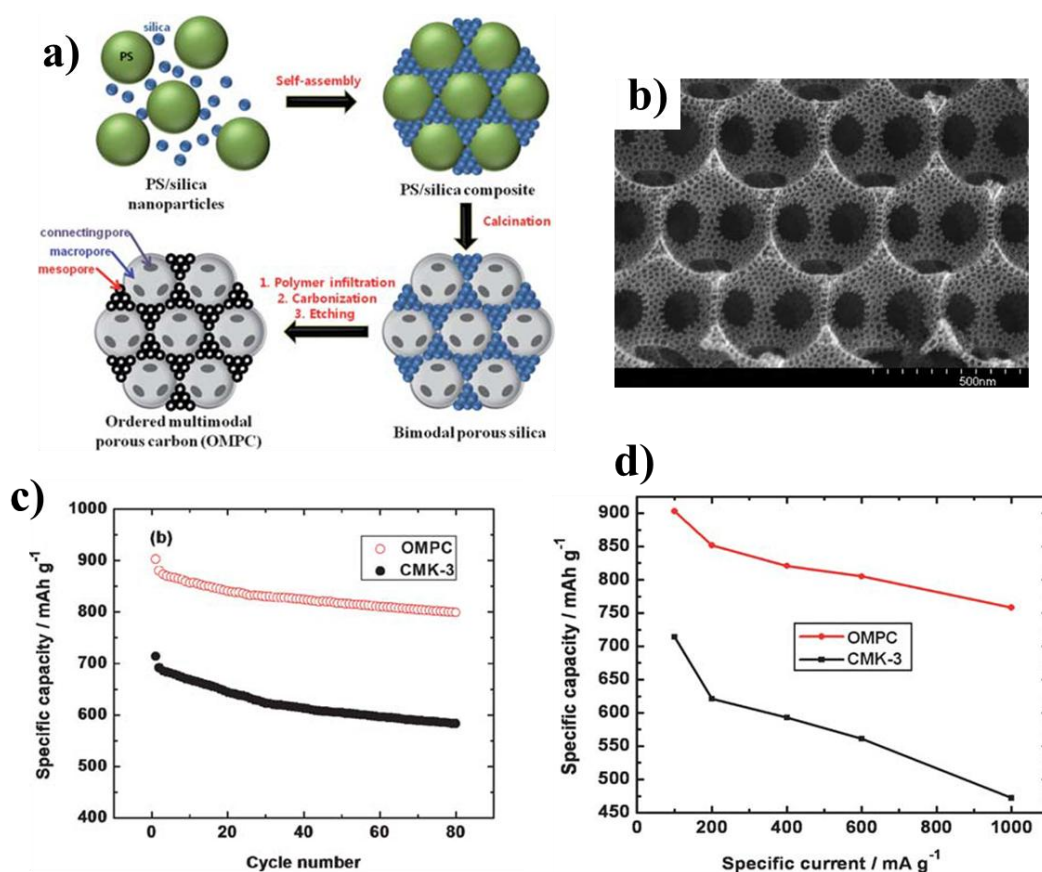


**Fig.10** a) Schematic representation for the preparation of ordered multimodal porous carbon (OMPC) via a dual-colloidal-templating approach. b) SEM image of the OMPC. c) Cycling- and d) rate performance of the OMPC in comparison with the ordered mesoporous carbon CMK-3. Adapted with permission from ref. 49.

To improve the LIB anode performance, much of the recent researches have been performed with the incorporation of metal oxide nanoparticles (e.g.,  $\text{Co}_3\text{O}_4$ ,  $\text{Fe}_3\text{O}_4$ ,  $\text{SnO}_2$ ,  $\text{MoO}_2$ , and many others) into the carbon matrix. For example, incorporation of  $\text{SnO}_2$  nanoparticles ( $<100 \text{ nm}$ ) into porous carbon prepared from RF gel could deliver a capacity of  $1300 \text{ mAh g}^{-1}$  after 450 discharge/charge

cycles and a capacity of  $180 \text{ mAh g}^{-1}$  even at a current density of  $4000 \text{ mA g}^{-1}$  with  $\sim 100\%$  Coulombic efficiency.<sup>50</sup>

Porous graphene networks with metal oxide nanoparticles have also been explored as electrode materials.  $\text{Fe}_2\text{O}_3$  nanoparticles-coated graphene network composites were simply prepared by annealing of MIL-88-Fe (a type of MOF) particles within the graphene network.<sup>33</sup> When evaluated as an anode material, the composite showed a reversible capacity of  $864 \text{ mAh g}^{-1}$  (approximately 76% of the initial capacity of  $1133 \text{ mAh g}^{-1}$ ) for 50 cycles at a current density of  $200 \text{ mA g}^{-1}$ . High rate capacity was also observed for this anode material (Fig. 11). There are also reports on incorporation of other types of nanoparticles into graphene network to improve electrode performance, *e.g.*,  $\text{MoS}_2$  nanoparticles.

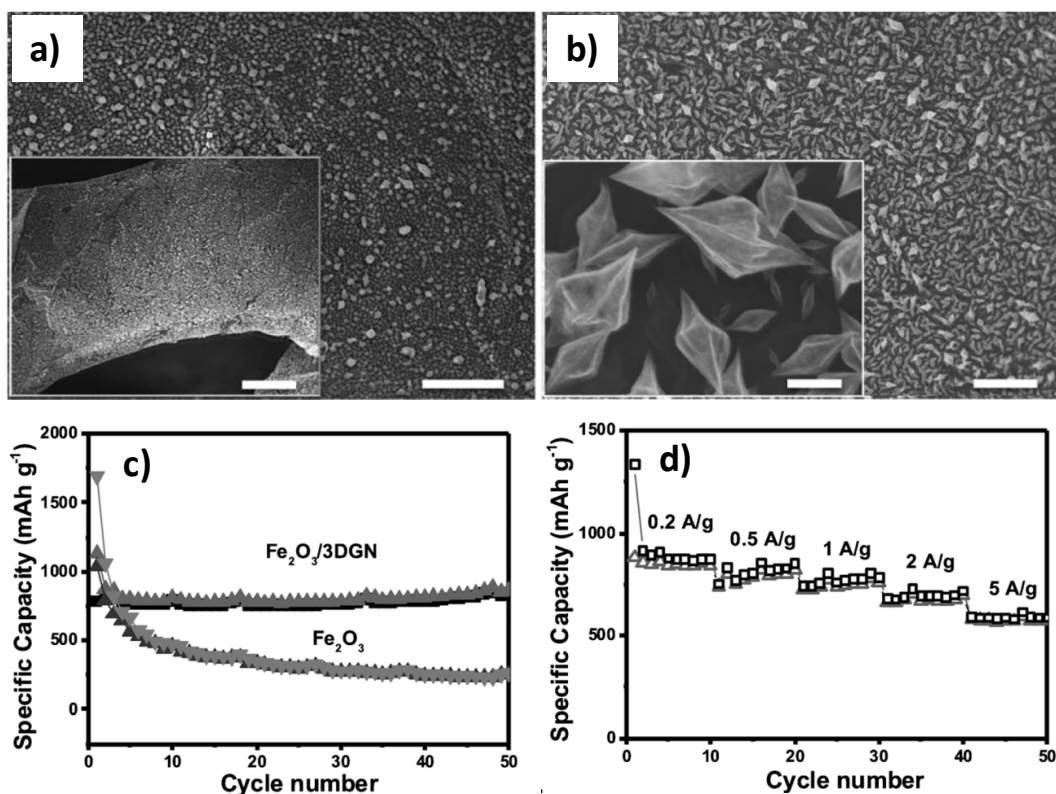


**Fig. 11** a) SEM image of MIL-88-Fe/graphene network composites, scale bar  $5 \mu\text{m}$ . Inset: low magnification SEM image, scale bar  $10 \mu\text{m}$ . b) SEM image of  $\text{Fe}_2\text{O}_3$  nanoparticles on graphene network, scale bar  $3 \mu\text{m}$ . Inset: high magnification SEM image with scale bar  $200 \text{ nm}$ . c) Cycling performance of the  $\text{Fe}_2\text{O}_3$  and  $\text{Fe}_2\text{O}_3$ -graphene composite at the current density of  $0.2 \text{ A g}^{-1}$ . d) Rate

capacity profile of the electrode made of Fe<sub>2</sub>O<sub>3</sub>-graphene composite. Adapted with permission from ref. 33. © 2014 Wiley-VCH.

## 7. Conclusions and Remarks

In summary, we have introduced the basics of lithium ion batteries and explained how the performance of the electrodes may be evaluated. The commonly used techniques for the preparation of carbon spheres, porous carbon monoliths, and the relevant composites are described. For the porous monoliths, we have focused on hierarchically porous structures with highly interconnected macropores, prepared by the methods including emulsion templating and ice templating. Some latest progress in fabrication of porous carbon materials are explained as well, *i.e.*, biomass as sustainable carbon precursors and metal-organic frameworks as templates. Among many applications, porous carbon materials have a wide range of applications for energy storage, *e.g.*, gas storage, supercapacitors, electrode materials for different types of batteries or catalytic reactions. This review has discussed that carbon spheres and porous carbon monoliths have great promise as potential alternative LIB anode materials. These materials have been prepared and demonstrated with high specific capacities, many of which outperform the maximum theoretical capacity for graphite (372 mAh g<sup>-1</sup>). Hierarchical porosity within these materials can lead to significantly improved rate capability. Problems such as high values for C<sub>irr</sub>, sloped voltage profiles, and in some cases poor cycle stability still need to be addressed, but investigations into carbon structure, porosity, morphology and surface chemistry may suggest solutions to these issues. Systematic studies on the relationship between these characteristics, processing parameters, and performance as electrode materials would be highly beneficial. High costs and complexity of fabrication procedures are also issues for some processes. However, attempts to design facile synthetic methodologies, such as the hydrothermal route for CS synthesis, and emulsion- and ice-templating routes for porous carbon monoliths, may provide low-cost and scalable pathways for production. However, in order to realize the full potential of monolithic electrodes, a big challenge for the production of crack-free and mechanically stable monoliths with desired composition and porosity must be addressed.

Although the examples demonstrated here for anode materials, it is obvious that the preparation techniques described here can be employed to fabricate suitable composite materials with desired pore morphology and nanostructures for more applications, *e.g.*, as cathode materials for lithium ion battery, as electrodes for Li-air and Li-S batteries, and other potential applications.<sup>1-7</sup> These materials are critical for numerous high-tech and emerging applications, such as in electric vehicles and stationary energy storage systems, and will receive increasing attention in the future. We believe that the continued exploration of such pathways will be a direction of growing importance for this field of research, since it is a critical requirement if the goal of wide-spread application and commercialisation is to be realised. In addition to energy storage applications, carbon materials in the format of monoliths and spheres have been widely used for supported catalysis, adsorbents, gas separation, and water treatment. In all these applications, the control of pore structure, pore volume, and pore size are critical. The mechanical stability and structure integrity during these applications are extremely important in order to maintain the materials performance and their recyclability. There is no doubt that the incorporation of doped elements, metal nanoparticles, metal oxide nanoparticles, and also surface functionalization, will also improve the performance of these materials for the above-mentioned applications. Thus, the synthetic methods discussed in this review can be employed to produce high performance carbons, carbon-based composites, and other types of materials for a much broader range of applications.

### Acknowledgement

AR is grateful for the joint PhD studentship between the University of Liverpool and Singapore A\*STAR.

### References

- 1 P. G. Bruce, S. A. Freunberger, L. J. Hardwick and J.-M. Tarascon, *Nature Mater.*, 2011, **11**, 19-29.
- 2 L. Ji, Z. Lin, M. Alcoutlabi and X. Zhang, *Energy Environ. Sci.*, 2011, **4**, 2682-2699
- 3 M. Winter, J. O. Besenhard, M. E. Spahr and P. Novák, *Adv. Mater.*, 1998, **10**, 725-763.

- 4 H. Nishihara and T. Kyotani, *Adv. Mater.*, 2012, **24**, 4473-4498.
- 5 A. Vu, Y. Qian and A. Stein, *Adv. Energy Mater.*, 2012, **2**, 1056-1085.
- 6 S. Nardecchia, D. Carriazo, M. L. Ferrer, M. C. Gutiérrez and F. del Monte, *Chem. Soc. Rev.*, 2013, **42**, 794-830.
- 7 A. Nieto-Márquez, R. Romero, A. Romero and J. L. Valverde, *J. Mater. Chem.*, 2011, **21**, 1664-1672.
- 8 M. Winter and R. J. Brodd, *Chem. Rev.*, 2004, **104**, 4245-4269.
- 9 J. -K. Park, *Principles and applications of lithium secondary batteries*, Wiley, Somerset, NJ, 2012.
- 10 C. H. Hamann, A. Hamnett and W. Vielstich, *Electrochemistry*, Wiley-VCH Verlag GmbH & Co., KGaA, Weinheim, 2<sup>nd</sup> edition, 2007.
- 11 J. R. Owen, *Chem. Soc. Rev.*, 1997, **26**, 259-267.
- 12 H. Zhou, S. Zhu, M. Hibino, I. Honma and M. Ichihara, *Adv. Mater.*, 2003, **15**, 2107-2111.
- 13 H. Qian, F. Han, b. zhang, Y. Guo, J. Yue and B. Peng, *Carbon*, 2004, **42**, 761-766.
- 14 Y. Z. Jin, C. Gao, W. K. Hsu, Y. Zhu, A. Huczko, M. Bystrzejewski, M. Roe, C. Y. Lee, S. Acquah, H. Kroto and D. R. M. Walton, *Carbon*, 2005, **43**, 1944-1953.
- 15 F. Su, X. S. Zhao, Y. Wang, L. Wang and J. Y. Lee, *J. Mater. Chem.*, 2006, **16**, 4413-4419.
- 16 X. Chen, K. Kierzek, Z. Jiang, H. Chen, T. Tang, M. Wojtoniszak, R. J. Kalenczuk, P. K. Chu and E. Borowiak-Palen, *J. Phys. Chem. C*, 2011, **115**, 17717-17724.
- 17 M. -M. Titirici, R. J. White, C. Falco and M. Sevilla, *Energy Environ. Sci.* 2012, **5**, 6796-6822.
- 18 X. Sun and Y. Li, *Angew. Chem. Int. Ed.*, 2004, **43**, 597-601.
- 19 Y. -S. Hu, R. Demir-Cakan, M. -M. Titirici, J. -O. Müller, R. Schlögl, M. Antonietti and J. Maier, *Angew. Chem. Int. Ed.*, 2008, **47**, 1645-1649.
- 20 J. B. Joo, P. Kim, W. Kim, J. Kim, N. D. Kim and J. Yi, *Curr. Appl. Phys.*, 2008, **8**, 814-817.
- 21 X. Sun and Y. Li, *J. Colloid Interface Sci.*, 2005, **291**, 7-12.
- 22 Z. -C. Yang, Y. Zhang, J. -H. Kong, S. Y. Wong, X. Li and J. Wang, *Chem. Mater.*, 2013, **25**, 704-710.
- 23 S. Yang, H. Zeng, H. Zhao, H. Zhang and W. Cai, *J. Mater. Chem.*, 2011, **21**, 4432-4436.

- 24 J. Liu, S. Z. Qiao, H. Liu, J. Chen, A. Orpe, D. Zhao and G. Q. Lu, *Angew. Chem. Int. Ed.*, 2011, **50**, 5947-5951
- 25 Y. Z. Jin, Y. J. Kim, C. Gao, Y. Q. Zhu, A. Huczko, M. Endo and H. W. Kroto, *Carbon*, 2006, **44**, 724-729.
- 26 H. Wang, T. Abe, S. Maruyama, Y. Iriyama, Z. Ogumi and K. Yoshikawa, *Adv. Mater.*, 2005, **17**, 2857-2860.
- 27 Y. Wang, F. Su, C. D. Wood, J. Y. Lee and X. S. Zhao, *Indu. Eng. Chem. Res.*, 2008, **47**, 2294-2300.
- 28 J. Xiao, M. Yao, K. Zhu, D. Zhang, S. Zhao, S. Lu, B. Liu, W. Cui and B. Liu, *Nanoscale*, 2013, **5**, 11306-11312
- 29 J. Kong, W. A. Yee, L. Yang, Y. Wei, S. L. Phua, H. G. Ong, J. M. Ang, X. Li and X. Lu, *Chem. Commun.*, 2012, **48**, 10316-10318.
- 30 M. He, L. Yuan, X. Hu, W. Zhang, J. Shu and Y. Huang, *Nanoscale*, 2013, **5**, 3298-3305.
- 31 W. -M. Zhang, J. -S. Hu, Y. -G. Guo, S. -F. Zheng, L. -S. Zhong, W. -G. Song and L. -J. Wan, *Adv. Mater.*, 2008, **20**, 1160-1165.
- 32 X. Cao, Y. Shi, W. Shi, G. Lu, X. Huang, Q. Yan, Q. Zhang and H. Zhang, *Small*, 2011, **7**, 3163-3168.
- 33 X. Cao, B. Zheng, X. Rui, W. Shi, Q. Yan and H. Zhang, *Angew. Chem. Int. Ed.*, 2014, **53**, 1404-1409
- 34 Y. Zhai, Y. Dou, D. Zhao, P. F. Fulvio, R. T. Mayes and S. Dai, *Adv. Mater.*, 2011, **23**, 4828-4850.
- 35 S. D. Kimmins and N. R. Cameron, *Adv. Funct. Mater.*, 2011, **21**, 211-225.
- 36 N. Cohen and M.S. Silverstein, *Polymer*, 2011, **52**, 282-287.
- 37 H. D. Asfaw, M. Roberts, R. Younesi and K. Edström, *J. Mater. Chem. A*, 2013, **1**, 13750-13758.
- 38 N. Brun, L. Edembe, S. Gounel, N. Mano and M. M. Titirici, *ChemSusChem*, 2013, **6**, 701-710.
- 39 N. Brun, S. R. S. Prabakaran, M. Morcrette, C. Sanchez, G. Pécastaings, A. Derré, A. Soum, H. Deleuze, M. Birot and R. Backov, *Adv. Funct. Mater.*, 2009, **19**, 3136-3145.
- 40 L. Qian and H. Zhang, *J. Chem. Technol. Biotechnol.*, 2011, **86**, 172-184.

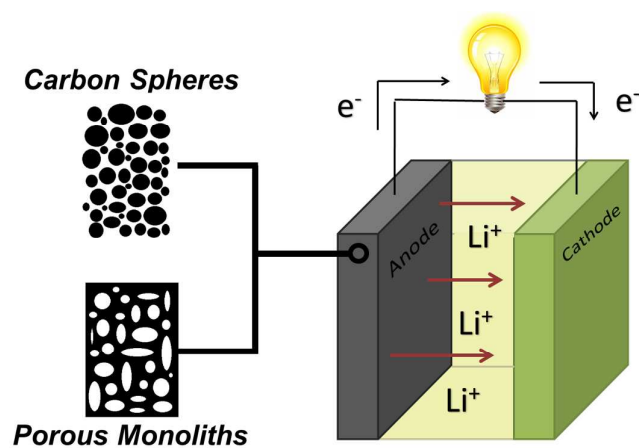
- 41 J. Spender, A. L. Demers, X. Xie, A. E. Cline, M. A. Earle, L. D. Ellis and D. J. Neivandt, *Nano Lett.*, 2012, **12**, 3857-3860.
- 42 L. Qian, E. Willneff and H. Zhang, *Chem. Commun.*, 2009, 3946-3948.
- 43 L. Estevez, R. Dua, N. Bhandari, A. Ramanujapuram, P. Wang and E. P. Giannelis, *Energy Environ. Sci.*, 2013, **6**, 1785-1790.
- 44 L. Qiu, J. Z. Liu, S. L. Y. Chang, Y. Wu and D. Li, *Nature Commun.* 2012, **3**:1241, 1-7
- 45 S. L. Candelaria, R. Chen, Y.H. Jeong and G. Cao, *Energy Environ. Sci.*, 2012, **5**, 5619 – 5637.
- 46 H. L. Jiang, B. Liu, Y. Q. Lan, K. Kuratani, T. Akita, H. Shioyama, F. Zong and Q. Xu, *J. Am. Chem. Soc.*, 2011, **133**, 11854-11857.
- 47 S. Lim, K. Suh, Y. Kim, M. Yoon, H. Park, D. N. Dybtsev and K. Kim, *Chem. Commun.*, 2012, **48**, 7447-7449.
- 48 Y. -S. Hu, P. Adelhelm, B. M. Smarsly, S. Hore, M. Antonietti and J. Maier, *Adv. Funct. Mater.*, 2007, **17**, 1873-1878.
- 49 B. Fang, M. -S. Kim, J. H. Kim, S. Lim, and J. -S. Yu, *J. Mater. Chem.*, 2010, **20**, 10253-10259.
- 50 Y. Xu, J. Guo and C. Wang, *J. Mater. Chem.* 2012, **22**, 9562 – 9567.

## ToC Graph

**Title:** Porous carbon spheres and monoliths: morphology controlling, pore size tuning and their applications as Li-ion battery anode materials

**Authors:** Aled D. Roberts, Xu Li and Haifei Zhang

Various synthetic techniques are employed to fabricate porous carbon spheres and monoliths for improved performance as Li-ion battery anode materials.





**Aled D. Roberts** grew up in a small village in North Wales before moving to study chemistry at the University of Liverpool, where he obtained his master's degree in 2012. He is currently undertaking a PhD study under the supervision of Dr. Haifei Zhang at the University of Liverpool and Dr Xu Li of the Institute of Materials Research and Engineering (IMRE) in Singapore. His project involves the fabrication and performance evaluation of novel porous carbon and carbon composite materials for energy storage applications. He is also a guest web-writer for the journal Energy and Environmental Science, and member of the 'Giving What We Can' organization.



**Dr Xu Li** is a senior scientist at Institute of Materials Research and Engineering (IMRE), A\*STAR, Singapore and an adjunct associate professor in Department of Chemistry, the National University of Singapore (NUS). He finished his PhD study in polymer chemistry at Department of Chemistry at NUS in 2001 and then joined in IMRE. He has published 67 papers with total citation times more than 1500 and H-index of 22. He also filed 12 patents. Dr Xu Li has been actively developing carbon nanomaterials for energy-related applications in the past few years.



**Dr Haifei Zhang** is a lecturer in the Department of Chemistry at the University of Liverpool since October 2010. He obtained his PhD in physical chemistry in the Institute of Chemistry, Beijing, in 2001. He was a postdoctoral researcher and then held a RCUK academic fellowship at the University of Liverpool in 2005-2010. He won the 12th Desty Memorial Award in 2007 for his innovative work in the manufacture of porous materials and their possible application in chromatography. His research interest is on porous polymers, nanostructured carbon materials, novel columns for chromatography and drug nanocrystals.

